SIMULATION OF SOLID FREEFORM FABRICATION

Stuart Brown

Department of Materials Science and Engineering
Massachusetts Institute of Technology
Cambridge, Massachusetts 02139

Abstract

Solid freeform fabrication involves highly coupled, nonlinear, thermomechanical processes. This investigation simulates the formation of a simple SFF geometry, a right, rectangular prism with aspect ratios of 1:1:2. We include the effects of material variation, deposition path, and initial conditions to predict resulting distortion.

Introduction

Most SFF processes are constrained in their range of application by certain mechanical and microstructural phenomena. Thermally-induced distortion limits the dimensional precision of these processes due to several inherent characteristics. First, the high temperature, local sintering or solidification zone produces large thermal gradients that in turn cause plastic deformation and distortion. Second, the subsequent shrinkage cooling of the high temperature and previously porous material introduce further distortion. Certain processes also introduce distortion due to differential cooling of a polymer stream.

In the case of 3D Printing, where the heating is primarily isothermal, distortion still results due to spatial variation in capillary forces developed between the binder and powder particles. This distortion can occur in certain extensions of SLS technology, where the laser is used to bind metal and ceramic powders coated with a thermoplastic binder. Distortion also results from the uneven shrinkage of the printed, porous green body during sintering. Finally, stereolithography can experience shrinkage due to the polymerization reaction [Iwanaga, et al., 1992; Weissman, et al., 1992].

This temperature-, polymerization- and binder-induced distortion also introduce residual stresses during processing. Cooling of a local high temperature zone surrounded by a lower temperature material introduces tensile stresses in the local zone. Unless removed, these tensile stresses can cause cracking and prevent the complete closure of pores. In some cases these tensile fields can introduce additional porosity by expanding smaller pores in the presence of a tensile hydrostatic state of stress.

These residual stress fields can act as the primary constraint on the application of components fabricated using any of these technologies. High strength requires low porosity and low residual stress states. The absence of either of these conditions significantly reduces the strength of any SFF component, as they would any porous body [Lakshminarayan and Marcus, 1992].

The relative amount of cohesion between different parts of fabricated components and the microstructure of components are deposition or sintering path dependent. Many nonlinear processes occur simultaneously in these technologies, for example: nonlinear thermal conduction, viscoplastic deformation, powder flow, grain growth, and capillary flow. Given these nonlinearities, it is very difficult to predict the best deposition/sintering path to produce a component with the least distortion and residual stress, and the best material properties.

The only work of which we are aware that has employed three dimensional modeling of any SFF technology is by Iwanaga [Iwanaga, et al., 1992], who appears to have used finite element analysis to simulate photolithography. Documentation of this Japanese effort is very limited, however. Hsu [Hsu, 1992] presents some preliminary simulation of sintering using finite element methods, but did not consider issues specific to transient SFF processes. Hsu also employed a rather simple constitutive model for sintering without including the effect of elasticity or residual stresses. To summarize, we are not aware of any three dimensional simulation of domestic SFF processes, including SLS and 3D Printing.

The following sections provide the details of the finite element analysis used to simulate the deposition of a right, rectangular prism. The effect of different materials, beam paths, initial conditions, and boundary conditions are given in the next section. The paper closes with discussion and conclusions.

Model Details

The finite element code ABAQUS is used to simulate a generic SFF process. Figure 1 illustrates the simple prism used in the analysis. The body is very small, consisting of 16 elements arranged in a prism with aspect ratios of 1:1:2. The body is held fixed at one corner and allowed to displace freely at all other points. Deposition and/or heating of powder material is simulated using an element activation capability in ABAQUS. Each beam path variation therefore activates elements in a different order. The simulation is a decoupled thermomechanical analysis, where the thermal history resulting from a thermal analysis is used as the loading for a subsequent mechanical analysis. The activation of elements in the mechanical analysis is delayed by one element activation step to activate elements in their high temperature state, thereby eliminating any mechanical effect due to heating of loose powder. All analyses were performed using a DECstation 5000.

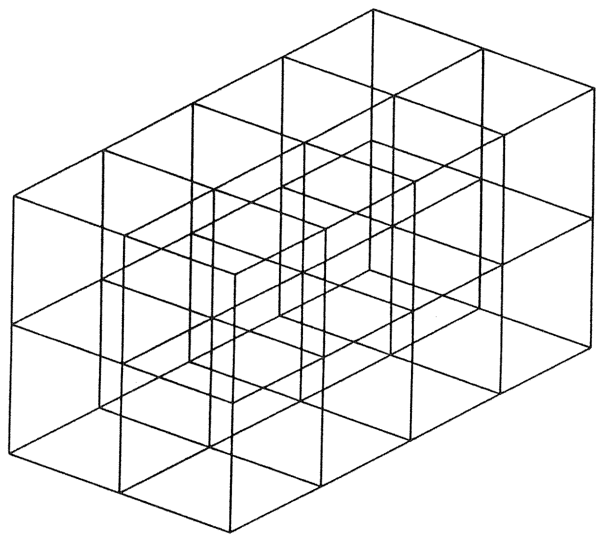

Figure 1 Finite element model of right, rectangular prism.

Two materials, a plain carbon steel and polycarbonate, were included in the analysis assuming elastic-plastic, rate-independent behavior. Our previous analyses of welding processes indicate that a rate-independent assumption works reasonably well for predicting metal distortion. The polycarbonate is most likely less accurately modeled using rate-independent models. Material properties (elastic moduli, specific heat, yield stress, thermal expansion coefficient, thermal conductivity) vary with temperature in the simulation. Behavior above the melting temperature was approximated by a very small value of yield stress.

The heating of the surface was simulated by the imposition of a uniform energy flux on the surface of a newly activated element. The magnitude of the flux was adjusted until the material within the element exceeded its melting temperature. Heat transfer is modeled approximately using film coefficients on the surfaces of the activated elements. Film coefficients were therefore assigned and eliminated as elements became activated and as elements were covered by previously unactivated elements.

The simulations did not include the effects of radiation heat transfer, rate-dependent constitutive behavior, orientation dependence of the heat transfer coefficient, powder constitutive behavior, or effects due to capillary flow.

Experimental Results

Figure 2 illustrates representative results for a simulation at different stages in the deposition of the full prism. This simulation employed steel constitutive behavior and deposited materials along the long axis of the prism. The dashed lines indicate the shape of the prism in the absence of any deformation. The solid lines indicate the shape of the prism at that stage. The final deformed shape corresponds to the final room temperature configuration.

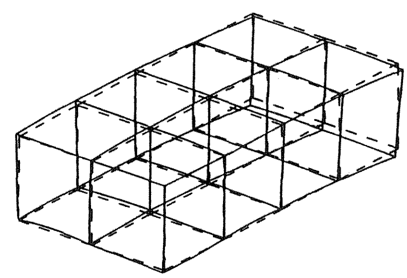

First layer deposited

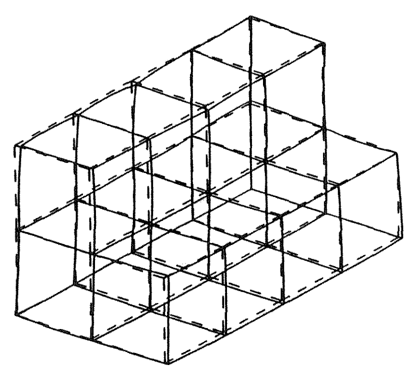

First row of second layer deposited

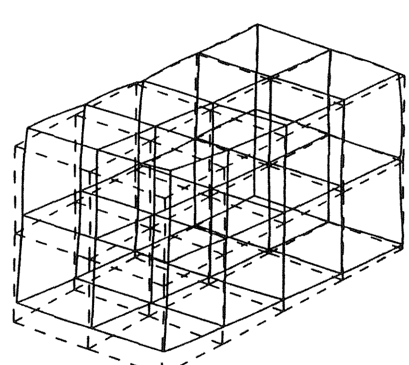

Final deposited geometry

Figure 2 Representative sequence of distortion resulting from steel prism simulation.

Table 1 summarizes the effect of different deposition (beam) paths and initial conditions for the steel deposition using the final, fully cooled, vertical displacement of a lower corner of the prism for comparison. The vertical displacement was much larger than displacements in the plane of deposition. The corner location is illustrated in figure 3. It is interesting that the simulations indicates that the path with the lower distortion also results in the lowest maximum principal tensile stress. Path selection therefore may offer promising opportunities in improving component properties. Increasing the ambient temperature (from 20 Celsius to 800 Celsius) produced significant reductions in residual stresses and displacements.

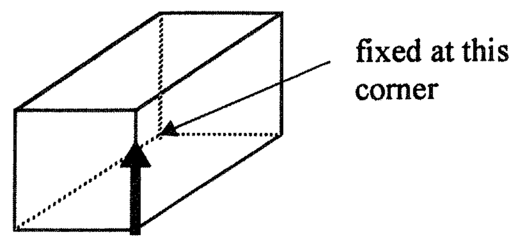

Figure 3 Location of point displacement used to compare different simulation cases.

Table 1: Comparison of beam paths and initial conditions

Simulation description	**Beam path in each layer**	**Corner vertical displacement**	**Maximum principal tensile stress**
Steel, beam path in one direction only along prism long axis.		0.12 mm	980 MPa
Steel, beam path in two directions along prism long axis.		0.12 mm	1000 MPa
Steel, beam path in one direction only along prism long axis.	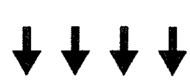	0.10 mm	860 MPa
Steel, beam path in one direction only along prism long axis, initial and ambient temperature of 800 Celsius.		0.05 mm	98 MPa

The effect of change in materials was unremarkable. Displacements associated with the polycarbonate prism were within a factor of two of those associated with the steel. However, the polycarbonate is first, rate-dependent and is second, highly dependent on the particular manufacturer's formulation. More accurate simulation of the polycarbonate therefore requires more accurate constitutive models for the polymer thermal and mechanical behavior.

Discussion and Conclusions

Given the guidance that such process modeling has provided to other processes, such as welding [Brown and Song, 1992], we expect even greater benefit to be derived in SFF. SFF processing is at a sufficiently early stage of maturity where many of the nonlinear process interactions are not well understood. We believe that accurate simulation capabilities will provide substantial assistance in understanding these nonlinearities.

The simulation work proposed here is not coupled to any one particular SFF technology, but instead is applicable to a number of SFF processes, including SLS, 3D Printing, Stereophotolithography and the Stratasys process. Consequently, the insights gained through this effort should assist the development of several competing processes.

Acknowledgments

This work was funded primarily by the Office of Naval Research (grant number N00014-90-J-1938). Additional support was provided by the Materials Processing Center at M.I.T. and the Richard P. Simmons Career Development Chair in the Department of Materials Science and Engineering.

References

1 Brown, S. and Song, H., "Implications of 3D Numerical Simulations of Welding of Large Structures," The Welding Journal, February 1992, pp. 55s-62s.

2 Brown, S. and Song, H., "Finite Element Simulation of Welding of Large Structures," Journal of Engineering for Industry, November 1992, pp. 441-451.

3 Cima, M., Sachs, E., Proceedings of the Solid Freeform Fabrication Symposium, University of Texas at Austin, 1991, pp. 187-194.

4 Cima, M., Lauder, A., Khanuja, S., Sachs, E., "Microstructural Elements of Components Derived from 3D Printing," Proceedings Solid Freeform Fabrication Symposium, August 3-5, 1992, University of Texas, Austin, Texas, pp. 220-227.

5 Crump, S.S., "The Extrusion Process of Fused Deposition Modeling," Proceedings, Third International Conference on Rapid Prototyping, June 7-10, 1992, University of Dayton, Ohio, pp. 91-100.

6 Hsu, M.B., "Numerical Simulation of Viscous Sintering under Mechanical Loads," Proceedings Solid Freeform Fabrication Symposium, August 3-5, 1992, University of Texas, Austin, Texas, pp. 188-195.

7 Iwanaga, S., Ohkawa, M., Igarashi, K., Kurihara, F., "Influence of Material Characterization on Dimensional Stability," Proceedings, Third International Conference on Rapid Prototyping, June 7-10, 1992, University of Dayton, Ohio, pp. 77-89.

8 Jacobs, P.F., "Rapid Prototyping and Manufacturing," Society of Mechanical Engineers, 1992.

9 Lakshminarayan, U. and Marcus, H.L, "An Experimental Study of the Relationship between Microstructure and Mechanical Properties of a Ceramic Composite Fabricated by Selective Laser Sintering," Proceedings Solid Freeform Fabrication Symposium, August 3-5, 1992, University of Texas, Austin, Texas, pp. 44-53.

10 Marcus, H.L., Beaman, J.J., Barlow, J.W. and Bourell, D.L., "From Computer to Component in 15 Minutes: Integrated Manufacture of Three Dimensional Objects," Journal of Metals, April, 1990, p. 8.

11 Weissman, P., Bolan, B., and Chartoff, R., "Measurements of Linear Shrinkage and the Residual Stresses Developed During Laser Photopolymerization," Proceedings, Third International Conference on Rapid Prototyping, June 7-10, 1992, University of Dayton, Ohio, pp. 103-112.